

1 Establishment and characterization of a tumoroid biobank derived 2 from dog patients' mammary tumors for translational research.

3
4 Antonella Raffo-Romero¹, Soulaimane Aboulouard¹, Emmanuel Bouchaert^{1,2}, Agata Rybicka^{1,2},
5 Dominique Tierny^{1,2}, Nawale Hajjaji^{1,3}, Isabelle Fournier^{1,4}, Michel Salzet^{1,4*†}, Marie Duhamel^{1*†}

6 ¹Université Lille, Inserm, CHU Lille, U1192, Laboratoire Protéomique, Réponse Inflammatoire et
7 Spectrométrie de Masse (PRISM), Lille, France

8 ²OCR (Oncovet Clinical Research), Parc Eurasanté Lille Métropole, 80 rue du Dr Yersin, 59120 Loos,
9 France

10 ³Breast Cancer Unit, Oscar Lambret Center, Lille, France

11 ⁴Institut Universitaire de France, Paris, France

12 *Corresponding authors: marie.duhamel@univ-lille.fr (MD), michel.salzet@univ-lille.fr (MS)

13 †MD and MS contributed equally to this work

14
15 **Keywords:** breast cancer, dog patients, tumoroid, biobank, drug screening

16 Abstract

17 Breast cancer is the most frequent cancer among women causing the greatest number of cancer-
18 related deaths. Cancer heterogeneity is a main obstacle to therapies. Around 96% of the drugs fail from
19 discovery to the clinical trial phase probably because of the current unreliable preclinical models. New
20 models emerge such as companion dogs who develop spontaneous mammary tumors resembling
21 human breast cancer in many clinical and molecular aspects. The present work aimed at developing a
22 robust canine mammary tumor model in the form of tumoroids which recapitulate the tumor diversity
23 and heterogeneity. We conducted a complete characterization of these canine mammary tumoroids
24 through histologic, molecular and proteomic analysis, demonstrating their strong similarity to the
25 primary tumor. We demonstrated that these tumoroids can be used as a drug screening model. In fact,
26 we showed that Paclitaxel, a human chemotherapeutic, could killed canine tumoroids with the same
27 efficacy as human tumoroids with 0.1 to 1 μ M of drug needed to kill 50% of the cells. Due to easy tissue
28 availability, canine tumoroids can be produced at larger scale and cryopreserved to constitute a
29 biobank. We have demonstrated that cryopreserved tumoroids keep the same histologic and
30 molecular features (ER, PR and HER2 expression) as fresh tumoroids. Two techniques of
31 cryopreservation were compared demonstrating that tumoroids made from frozen tumor material
32 allowed to maintain a higher molecular diversity. These findings revealed that canine mammary
33 tumoroids can be easily generated at large scale and can represent a more reliable preclinical model
34 to investigate tumorigenesis mechanisms and develop new treatments for both veterinary and human
35 medicine.

39 1 Introduction

40 A major obstacle in preclinical drug development for cancer is the lack of appropriate cell culture model
41 systems. Two-dimensional cancer cell lines are frequently used for the first screening of newly
42 developed drugs and for the study of cancer development. However, cancer cell lines completely lack
43 interaction with the tumor microenvironment, which is the main reason for drug resistance. Mouse
44 models present also several drawbacks leading to difficulties in the translation to human diseases. Such
45 models do not fully recapitulate the diversity and architecture of the primary disease, thus providing
46 inaccurate analysis of tumor pathogenesis and sensitivity to therapy. Around 96% of the drugs fail from
47 discovery to the clinical trial phase, probably because the preclinical models are not close enough to
48 the tumor biology in patients(1).

49
50 Tumoroid cultures represent a robust three-dimensional (3D) *in vitro* system that faithfully
51 recapitulate the genetic and phenotypic characteristics of the tumor from which they are derived. The
52 3D tumoroid system has been utilized to study different types of cancers(2–5). Tumoroids can serve to
53 better understand the biology but also to test drug efficacy *in vitro* before clinical trials in human
54 patients. Most of the tumoroid studies have been conducted on mouse and human tissue samples.
55 Mouse tumor tissues do not fully recapitulate the human disease and therefore are not the best
56 models for human translation. On the other hand, the use of human samples is the optimal solution
57 but the difficulty to access to the fresh tissues and ethical issues can slow down the large scale
58 screening of new drugs. That is why it is of prime importance that new models emerge than can fully
59 and faithfully recapitulate the human disease. Moreover, as tumoroids are found to have more and
60 more relevance and applications, large scale production of tumoroids become inevitable but presents
61 many challenges due to the difficulty of accessing large quantities of human fresh tissue.

62 In that regard, companion dogs with spontaneous tumors present a unique, ethical, non-experimental
63 model for comparative research and drugs development(6,7). Canine mammary tumor (CMT) is the
64 third most common type of cancer in dogs, and first in bitches with an incidence of around 230 cases
65 per 100,000 dogs per year(8–10). It possesses several advantages over highly inbred and genetically
66 modified laboratory animals, such as clinical profile (age at onset, predominance of carcinomas, and
67 type of metastases), genetics (role of BRCA1/2, overlapping gene signature) and molecular similarities
68 with its human counterpart(11,12). CMT, the same as human breast cancer (BC), can be characterized
69 by expression of estrogen, progesterone and HER2 receptors. The involvement of companion dogs
70 with spontaneous CMT in translational oncology is already seen in numerous publications and several
71 ongoing clinical trials(13). Canine tumoroids developed from dog patients with spontaneous CMT could
72 therefore provide a more representative and ethical translational model to test drug efficacy and
73 toxicity in pre-human studies, as well as canine tumoroids could be an innovative screening tool in
74 drug discovery, while reducing the number of experimental animals needed for *in vivo* studies. Few
75 canine tumoroids studies have been made so far(14–17), one of them has developed tumoroids from
76 canine normal and tumor breast stem cells(18). None of them have developed tumoroids from CMT
77 heterogeneous tissue recapitulating the tumor microenvironment.

78
79 The enormous potential of tumoroids as preclinical models has given rise to the development of
80 tumoroid biobanks. Tumoroid biobanks have been obtained from various tumor tissues(19). However,
81 there is a lack of knowledge about cryopreservation procedures and whether the cryopreserved
82 tumoroids maintain similar molecular and functional features as their fresh counterparts.

83 In this study, we have developed for the first time tumoroids from heterogeneous canine mammary
84 tumor tissues. We have demonstrated morphologic, histologic and molecular stability between fresh
85 CMT tumoroids and cryopreserved tumoroids. However, tumoroids made from frozen CMT material
86 show more similarities with fresh tumoroids compared to cryopreserved tumoroids. Treatment with a
87 chemotherapeutic drug also confirmed these results. Taken together, our study aimed at creating and

88 characterizing a new biobank of canine mammary tumoroids with similar features as human tissues
89 which can be used for large scale drug screening in preclinical studies.

90 **2 Materials and Methods**

91 **2.1. Human and Dog patients' tissue collection**

92 This study was carried out with canine mammary tumors (n = 6). The tumors were collected at different
93 veterinary clinics from dogs undergoing scheduled surgery. The samples were delivered with the
94 written consent of the owners. The dogs included in the study were treated surgically by their
95 veterinarian, and none of them received any additional treatment before the mastectomy. A
96 veterinary pathologist reviewed the tissue blocks to confirm the diagnosis and define the lesions for
97 dissection. For this study, we received a piece of fresh tumor of approximately 1 cm³.

98 Human breast tumor tissue was obtained from a patient undergoing surgery for early breast cancer.
99 Fresh tumor tissue was provided by the pathologist for organoid culture. The sample was anonymized
100 prior to its transfer to the lab. The study was approved by the local research committee of Oscar
101 Lambret Cancer center and a French Ethical Committee (study IdRCB 2021-A00670-41). The written
102 informed consent for the study was obtained from the patient before any procedure.

103 **2.2. Tissue processing**

104 Each tumor sample was divided into three pieces: one piece was snap frozen in liquid nitrogen before
105 being stored at -80°C for proteomics large scale study, the second piece was fixed in formaldehyde 4%
106 for 24h followed by dehydration in 20% sucrose for 24h, embedding in gelatin and storage at -80°C for
107 histopathological analysis and hematoxylin and eosin staining. The last tumor fragment was used for
108 tumoroids culture. For this, the tumor fragment was minced into 1 mm³ pieces before its enzymatic
109 digestion as described below.

110 **2.3. Tumoroid culture**

111 The minced tumor tissue was digested in 2 mL Hank's Balanced Salt Solution (HBSS, Gibco) with
112 antibiotics and anti-fungal (1X Penicillin/Streptomycin, 1X Amphotericin) containing 1 mg/mL
113 collagenase type IV (Sigma) and 5 U/ mL hyaluronidase (Sigma) at 37 °C for 2 h. During this time, the
114 medium containing the tumor tissue was mixed every 15 minutes to help digestion. After 2 h, 10 mL
115 of HBSS with antibiotics were added and the cell suspension was strained over a 100 µm filter (Dutcher)
116 which retained remaining tissue pieces. The suspension was centrifuged at 300 g for 5 minutes. In case
117 of a visible red pellet, erythrocytes were lysed in 1 mL red blood cell lysis buffer (RBC, Invitrogen) for 5
118 min at room temperature. Then, the suspension was completed with 10 mL HBSS with antibiotics and
119 centrifuged at 300 g for 5 minutes. The viable cell suspension was counted and 150,000 cells were used
120 for the generation of tumoroids. The cells were resuspended in a reduced growth factor solubilized
121 basement membrane matrix for Organoid Culture (Matrigel®, Corning) and plated as a drop in 24-well
122 plates. The matrigel was allowed to solidify for 30 minutes in the incubator and then 500 µl of complete
123 culture medium was added. The culture me-dium was composed of Advanced DMEM (Gibco)
124 supplemented with 1X Glutamax, 10 mM Hepes, 1X Penicillin/Streptomycin, 1X Amphotericin,
125 50µg/mL Primocin, 1X B27 supplement, 5 mM Nicotinamide, 1.25 mM N-Acetylcystein, 250 ng/mL R-
126 spondin 1, 5 nM Heregulinβ-1, 100 ng/mL Noggin, 20 ng/mL FGF-10, 5 ng/mL FGF-7, 5 ng/mL EGF, 500
127 nM A83-01, 500 nM SB202190 and 5µM Y-27632.

128 Tumoroids were split when confluent. Ice cold PBS was used to harvest tumoroids from the Matrigel.
129 They were collected in a 15 mL falcon that was pre-coated with PBS containing 1 % BSA solution to
130 prevent the tumoroids from adhering to the tube. The tumoroids were centrifuged at 300 g for 5

131 minutes and then digested with TrypLE solution (Gibco) for 5 min at 37 ° C. After enzymatic
132 neutralization and washing, the tumoroid fragments were resuspended in Matrigel and reseeded as
133 explained above to allow formation of new tumoroids.

134 Furthermore, after the initial digestion of the tumor tissue, 2 million cells were cryopreserved for the
135 subsequent development of tumoroids. To create the tumoroids from the frozen cells, the vial was
136 thawed slowly and the cells were centrifuged in 10 mL of HBSS with antibiotics at 300 g for 5 minutes.
137 Then, the cells were counted and seeded in the same way as with fresh cells.

138 **2.4. Freezing and thawing of tumoroids**

139 Once the tumoroids were confluent, they were collected as described before, centrifuged at 300 g for
140 5 minutes, separated with a syringe mounted with a 21 G needle before being centrifuged again and
141 frozen in 90% fetal bovine serum (FBS) and 10% DMSO.

142 Cryopreserved tumoroids were thawed slowly and 1mL of the thawing solution was added to the vial
143 (Advanced DMEM (Gibco), 15 mM HEPES (Gibco), 1 % BSA (Sigma)). Then, the solution was transferred
144 to a tube containing 2 mL of thawing solution. The tumoroids were centrifuged at 300 g for 5 minutes
145 and the pellet of tumoroids was resuspended with 30 µl of Matrigel and cultured as explained before.

146 **2.5. HE, Immunohistochemistry and Immunofluorescence staining**

147 The tumoroids were fixed in 2% paraformaldehyde with 0.1% glutaraldehyde for 24 h followed by
148 dehydration in 20% sucrose for 24 h, embedding in gelatin and freezing at -80°C.

149 Standard H&E staining was carried out on 5 µm thick tumor and tumoroid sections to appreciate the
150 cellular and tissue structure details, using Tissue-Tek Prisma® Automated Slide Stainer. Images were
151 acquired on a Nikon Eclipse NI-U with the Nikon Elements BR 4.50.00 software.

152 The immunohistochemical staining was carried out on 5 µm thick tumor and tumoroid sections using
153 an automated protocol developed for the Discovery XT automated slide staining system (Ventana
154 Medical Systems, Inc.). Tumor and tumoroid sections were incubated for 40 min with the appropriate
155 antibody before incubation with Discovery UltraMap anti-Rabbit (760–4315, Roche) or anti-mouse
156 horseradish peroxidase (HRP) (760–4313, Roche) secondary antibodies and the Discovery ChromoMap
157 DAB kit reagents (760–159, Roche). Counterstaining and post-counterstaining were performed using
158 hematoxylin and bluing reagent (Ventana, Roche Diagnostics). The following commercially available
159 antibodies were used for the characterization: estrogen receptor (ER)–α (SC-8005, Santa Cruz),
160 progesterone receptor (PR) (790–4296, Roche) and human epidermal growth factor 2 (HER-2) (790–
161 4493, Roche).

162 The immunofluorescence staining was carried out on 12 µm thick tumor and tumoroid sections. Tumor
163 and tumoroid sections were washed 3 times in PBS, pre-incubated in blocking buffer in 0.3% Triton,
164 5% Normal Donkey Serum (NDS) and 2% ovalbumin in PBS for 1 h at room temperature. Then the
165 samples were incubated overnight at 4 °C with proliferation marker Ki67 (790–4286, Roche). After 3
166 washes with PBS, samples were incubated 1 h at 37 °C with secondary donkey anti-rabbit antibody
167 conjugated to Alexa Fluor 488 (1:200, Invitrogen, Carlsbad CA, USA) in blocking buffer. They were
168 rinsed with PBS and the cell nuclei were counterstained with Hoechst 33342 fluorescent dye (1/10000,
169 Invitrogen, Carlsbad CA, USA) for 20 min at 4 °C. Finally, the tumor and tumoroid sections were
170 mounted on the slide with Dako Fluorescent Mounting Medium (Agilent, Santa Clara CA, USA). Samples
171 without the addition of primary antibody were used as negative control. The presented pictures are
172 representative of independent triplicates.

173 **2.6. Total protein extraction**

174 Sections of fresh frozen tumor and corresponding tumoroids were collected in triplicate for each
175 condition. The tumor sections and the tumoroids pellet were lysed with RIPA buffer (150 mM NaCl, 50
176 mM Tris, 5 mM EGTA, 2 mM EDTA, 100 mM NaF, 10 mM sodium pyrophosphate, 1% NP40, 1 mM
177 PMSF, and 1X protease inhibitors) for total protein extraction. Three steps of 30 seconds sonication at
178 amplitude 50% on ice was applied, cell debris were removed by centrifugation (16,000 × g, 10 min,
179 4°C), the supernatants were collected and protein concentrations were measured using a Bio-Rad
180 Protein Assay Kit, according to the manufacturer's instructions. To normalize the tumoroids and tumor
181 protein quantities, 100 µg of each sample was used for protein digestion and subsequent shotgun
182 proteomics analysis.

183 **2.7. Shotgun proteomics**

184 Protein digestion was performed using the FASP method(20). Briefly, reduction solution was added to
185 the sample (100 mM DTT in 8 M urea in 0.1 M Tris / HCl, pH 8.5 (UA buffer)) and incubated for 15
186 minutes at 95°C. The protein solution was then loaded onto 10 kDa Amicon filters, supplemented with
187 200 µL of UA buffer and centrifuged for 30 min at 14,000 g. Next, 200 µL of UA buffer were loaded
188 onto the filter and centrifuged for 30 min at 14,000 g. Then, 100 µL of alkylation solution (0.05 M
189 iodoacetamide in UA buffer) were added and incubated for 20 min in the dark before centrifugation
190 for 30 min at 14,000 g. Finally, a 50 mM ammonium bicarbonate solution (AB) was added and
191 centrifuged again for 30 min at 14,000 g. This last step was repeated three time. For the digestion, 50
192 µL LysC/Trypsin at 20 µg/mL in AB buffer was added and incubated at 37°C overnight. The digested
193 peptides were recovered after centrifugation for 30 min at 14,000 g. Then, two washes with 100 µL of
194 AB buffer were performed by centrifugation for 30 min at 14,000 g. Finally, the eluted peptides were
195 acidified with 10 µL of 0.1% trifluoroacetic acid (TFA) and dried under vacuum.

196 **2.8. LC-MS/MS analysis**

197 The samples once dried were reconstituted in 20 µL of a 0.1% TFA solution and desalted using a C18
198 ZipTip (Millipore, Saint-Quentin-en-Yvelines, France). After elution with 20 µL of 80 % acetonitrile
199 (ACN)/ 0,1 % TFA, the peptides were vacuum dried. Samples were then reconstituted in 0.1 % formic
200 acid/ACN (98:2, v/v), and separated by reverse phase liquid chromatography by an Easy-nLC 1000
201 nano-UPLC (Thermo Scientific) in the reverse phase using a preconcentration column (75 µm DI × 2
202 cm, 3 µm, Thermo Scientific) and an analytical column (Acclaim PepMap C18, 75 µm ID × 50 cm, 2 µm,
203 Thermo Scientific) interfaced with a nanoelectrospray ion source on an Q-Exactive Orbitrap mass
204 spectrometer (Thermo Scientific). Separation was performed using a linear gradient starting at 95 %
205 solvent A (0.1% FA in water) and 5 % solvent B (0.1% FA in ACN) up to 70 % solvent A and 30 % solvent
206 B for 120 min at 300 nL/min. The LC system was coupled onto a Thermo Scientific Q-Exactive mass
207 spectrometer set to Top10 most intense precursors in data-dependent acquisition mode, with a
208 voltage of 2.8 kV. The survey scans were set to a resolving power of 70 000 at FWHM (m/z 400), in
209 positive mode and using a target AGC of 3E+6. For the shotgun proteomics, the instrument was set to
210 perform MS/MS between +2 and +8 charge state.

211 **2.9. Data analyses**

212 All the MS data were processed with MaxQuant (version 1.5.6.5) software(21) using the Andromeda
213 search engine(22). Proteins were identified by searching MS and MS/MS data against a database of
214 *Canis lupus familiaris* obtain from Uniprot database and containing XXX sequences. For identification,
215 the FDR at the peptide spectrum matches (PSMs) and protein level was set to 1%. Label-free
216 quantification of proteins was performed using the MaxLFQ algorithm with the default parameters.
217 Analysis of the proteins identified were performed using Perseus (version 1.5.6.0) software(23,24).

218 Multiple-sample tests were performed using ANOVA test with a p-value of 5% and preserving grouping
219 in randomization. Visual heatmap representations of significant proteins variation were obtained using
220 hierarchical clustering analysis. Functional annotation and characterization of identified proteins were
221 obtained using PANTHER (version 13.0) software(25) and STRING (version 9.1)(26). The analysis of gene
222 ontology, cellular components and biological processes, were performed with FunRich 3.0 analysis
223 tool(27).

224 **2.10. Tumoroid response to Paclitaxel**

225 For tumoroid culture and drug response analysis, the same amount of tumoroids was dissociated with
226 cold PBS. The pellet was then digested with TrypLE solution (Gibco) for 5 min at 37 ° C. The tumoroids
227 were then diluted in HBSS and then passed through a 100 µm filter (Dutcher) to remove large
228 tumoroids. Subsequently, the tumoroids were centrifuged at 300 g for 5 minutes and then suspended
229 in 2% Matrigel/tumoroid culture medium (3-5000 tumoroids/mL). For the drug response, 100 µl of
230 tumoroid solution was placed in wells of 96-well plates coated with 1.5 % agarose. The tumoroids were
231 allowed to form during 72h and then treated with Paclitaxel for 7 days before performing the viability
232 test. Cell viability was performed using CellTiter-Glo 3D (Promega) according to the manufacturer's
233 instructions and results were normalized to controls. Paclitaxel concentrations ranged from 0.01 µmol
234 to 100 µmol (5 concentrations) and DMSO controls were added. After 7 days, 100 µL of CellTiter-
235 Glo3D reagent (Promega, Madison, WI, USA) was added to each well and the plate was shaken at
236 room temperature for 25 min. Luminescence was read on a TriStar2 S LB 942 Multimode Microplate
237 Reader and the data were analyzed using GraphPad Prism 6.

238 **3 Results**

239 **3.1. Feasibility of tumoroid culture from freshly resected canine mammary tumors**

240 Canine mammary tumor was collected in the operating room at the time of tumor resection. For the
241 characterization of the tumoroids' cultures, 6 on 31 patients of the established biobank were included
242 (**Supplementary Table 1**). For all of them, the resection was a primary mammary tumor. Patient's age
243 ranged between 5 and 14 years old and were all female. Based on the 2010 histologic classification for
244 canine mammary tumors, the 6 tumors were annotated (**Supplementary Table 1**)(28). The 6 tumors
245 were characterized with the most important and frequent biomarkers of breast cancer: estrogen
246 receptor (ER), progesterone receptor (PR) and HER2. Among the 6 tumors, 4 have a triple-negative
247 signature, signifying the absence of HER2, ER, and PR proteins expression (TM-02, TM-03, TM-05, TM-
248 06) while 2 tumors are of luminal subtype with PR expression (TM-01) or PR/ER expression (TM-04)
249 (**Supplementary Figure 1 and Supplementary Table 1**). In addition, the positive Ki67 labeling of each
250 tumor was evaluated. We found that all 6 tumors showed Ki67 positive cells, with variable levels
251 (**Supplementary Figure 2**).

252 After tumor resection, the tumor fragment was divided into three pieces: the first piece was kept fresh
253 for tumoroid culture generation, the second one was frozen without prior fixation and the last piece
254 was fixed in PFA and cryopreserved (**Figure 1A**). Frozen tissue was used for proteomics while fixed
255 tissue was used for histology.

256 Fresh tissue pieces were mechanically and enzymatically dissociated to obtain single cell suspensions
257 which were plated in Matrigel drops and overlaid with optimized mammary tumoroids culture
258 medium. Cultures were followed by microscopy for evidence of tumoroids formation. We successfully
259 generated tumoroid cultures from 31 of 33 tumor samples, an establishment success rate of 94%, with
260 long-term expansion. Indeed, all tumoroids were grown for at least 42 days (6 passages) (**Figure 1B**).
261 Majority of tumoroid lines were cryopreserved. The tumoroids morphologically reflected the original

262 tumor they were derived from (**Figure 1C**). Tumoroids presented patient-specific heterogeneous
263 morphologies, ranging from compact structures (TM-02) to more irregularly structures (TM-03 and
264 TM-04).

265 **3.2. Canine mammary tumoroids can be generated from both fresh and frozen cells and can be** 266 **cryopreserved with similar histological and molecular features.**

267 Next, we wanted to evaluate whether tumoroids could be generated from frozen cells while keeping
268 the same characteristics as fresh tumoroids. From the primary tumor sample, we divided the cell
269 suspension into two parts: one part kept fresh for direct tumoroid formation, named “Fresh
270 tumoroids” thereafter and the second part was frozen for indirect tumoroid formation, named
271 “Tumoroids from frozen cells” thereafter. In addition, in order to characterize our biobank, we wanted
272 to make sure that cryopreservation did not affect the tumoroids features. We therefore compared
273 these two types of tumoroid cultures to thawed tumoroids, named “Frozen tumoroids” thereafter
274 (**Figure 2A**). Tumoroids from these different culture conditions were left in culture during 4-5 weeks
275 (date 1) or 6-7 weeks (date 2) and compared to study tumoroids drift overtime.

276 Histologic and molecular drifts of tumoroids after cryopreservation and after long-term culture were
277 studied. First, the culture of tumoroids was successful for each culture condition and after serial
278 passages as well (**Figure 2B**). Tumoroid formation efficiency was not found to be different between
279 cryopreserved cells and fresh cells. Tumoroid cultures from fresh and frozen cells could be similarly
280 long-term cultured and passaged (**Figure 2B**). At the histological level, tumoroids derived from fresh
281 cells, frozen cells or after cryopreservation retained the same architecture. **Figure 2C** presents
282 representative images of H&E staining of tumoroids derived from two different tumors. Tumoroids
283 derived from TM-02 were compact while tumoroids derived from TM-03 were more irregular whatever
284 the culture condition and time in culture. The freezing procedure did not affect tumoroids morphology.

285 The ER, PR and HER2 expression profiles of breast cancer tumoroids were compared with their original
286 breast cancer tissues. For this, 2 tumors were used: TM-03 (triple negative subtype) and TM-04
287 (luminal subtype) (**Figure 3**). The results showed that the tumoroids maintain the same expression
288 profile of the tumor of origin. In the case of TM-03, tumoroids present a triple negative subtype as the
289 tumor they are derived from. In the case of TM-04 tumoroids, we can observe ER and PR positive cells
290 similar to the tumor of origin.

291 Finally we verified if the proliferation of the tumoroids in all three conditions was similar. We used the
292 TM-05 tumoroids that show a large number of positive cells in the tumor of origin (**Supplementary**
293 **Figure 2**) to answer this question. The proliferative activity of the tumoroids was determined by the
294 percentage of Ki67+ cells with respect to the total cells of each tumoroids conditions. Proliferation
295 activity of tumoroids do not show a significant difference between Fresh (8.61%), Frozen (6.96%) and
296 FrozenCell (6.29%) tumoroids (**Figure 4**).

297 **3.3. Similar proteomic profiles are observed between tumoroids generated from fresh and frozen** 298 **cells over time while cryopreservation seems to trigger a more pronounced molecular drift.**

299 We have shown that the freezing procedure as well as the passages did not impact the morphology of
300 tumoroids neither their histological features. In order to understand, whether the frozen tumoroids or
301 tumoroids made from frozen cells kept similar molecular profiles as the fresh tumoroids or the original
302 tumor, we have performed a large-scale unbiased proteomic analysis. The study was carried out on 3
303 tumors: TM-01, TM-02 and TM-03; of which the three types of tumoroids were made and compared
304 with each other, and with the original tumor. For this the extracted proteins were quantified and the
305 same amount of proteins was used. In addition, to understand if there was any molecular drift over

306 time, we have analyzed the proteome of tumoroids at two different dates. More than 2,500 proteins
307 were identified in total through biological replications within the experimental groups.

308 First, taking into account the two dates of tumoroid passage (D1 and D2), 1796 proteins were identified
309 shared by the six conditions; D1-Fresh, D1-FrozenCell, D1-Frozen, D2-Fresh, D2-FrozenCell and D2-
310 Frozen (62% of all the proteins identified) (**Figure 5A**) (**Supplementary Table 2**). The D1-Frozen
311 tumoroids seem to be the most different compared to all the other conditions as shown on **Figure 5A**.
312 In fact, 343 proteins were identified in all conditions except in D1-Frozen. This may be due to a lack of
313 protein diversity in this condition, as all samples were quantified to have the same amount of proteins.
314 However, if we observed more closely the proteins lacking in the condition of D1-Frozen (**Figure 5B**),
315 we found several proteins involved in metabolism and energy pathways such as HMGCS2
316 (Hydroxymethylglutaryl-CoA synthase), SOAT1 (Sterol O-acyltransferase 1), PRPSAP1 (Phosphoribosyl
317 pyrophosphate synthase-associated protein 1), ECI1 (Enoyl-CoA delta isomerase 1), MMP9 (Matrix
318 metalloproteinase-9), UBE4B (Ubiquitin conjugation factor E4 B), BMP1 (Bone morphogenetic protein
319 1) and HEXB (Beta-hexosaminidase subunit beta) among many others. In addition, we found proteins
320 involved in the inhibition of apoptosis such as API5 (Apoptosis Inhibitor 5), SOD2 (Superoxide
321 dismutase 2), SYVN1 (Synoviolin 1). We also identified a lot of proteins involved in Cell growth and/or
322 maintenance and Cell communication. Very interestingly, proteins involved in immune response
323 processes were enriched such as NRP1 (Neuropilin 1), PROCR (Protein C Receptor-CD201), ALCAM
324 (activated leukocyte cell adhesion molecule-CD166), CD109 (Cluster of Differentiation 109), LBP
325 (Lipopolysaccharide-binding protein), ST6GAL1 (ST6 Beta-Galactoside Alpha-2,6-Sialyltransferase 1),
326 LRRC8A (Leucine-rich repeat-containing protein 8A) and CFB (Complement Factor B). These proteins
327 which were not found in the D1-Frozen condition have a proliferative, immune and anti-apoptosis
328 profile; demonstrating a lack of these biological processes in the D1-Frozen condition.

329 Likewise by a Pearson correlation analysis, hierarchical clustering of all the samples based on the
330 correlation coefficients between them revealed higher similarity between Fresh and Frozen Cell
331 tumoroids at date 1 and 2. Frozen tumoroids were more different, specifically at date 1 (**Figure 5C**).
332 The similarity of D1-Frozen with the other conditions was less than 87% while all the other conditions
333 showed more than 95% similarity. The duration of the tumoroids culture did not seem to have a big
334 impact on their proteomic profiles. The fact that D1-Frozen tumoroids were more distinct suggests
335 that the tumoroids should be preferentially left in culture long enough to recover after freezing, which
336 was not observed from D1-FrozenCells.

337 Knowing that the time in culture did not impact too much their molecular profile, we then wanted to
338 verify whether the culture condition impacted or not their proteome. For that, we have compared the
339 proteomic profiles of tumoroids from three culture conditions: fresh, frozen and tumoroids made from
340 frozen cells. First of all, the principal component analysis (PCA) based on the LFQ values of the protein
341 identification showed that the samples were grouped by tumor and not according to the type of
342 culture condition (**Figure 5D**). This sample grouping by PCA means that there was a high level of
343 similarity between the biological replicates of each condition but also between the tumoroids without
344 influence of their culture condition. Furthermore, a Venn diagram showing the number of common
345 and unique proteins in all conditions showed that a majority of proteins were identified in all three
346 conditions of culture (2389 proteins, representing 90% of all proteins). However, some proteins were
347 found specifically expressed in each condition: 27 identified specifically in fresh tumoroids, 23 in frozen
348 tumoroids and 34 in tumoroids made from frozen Cells (**Figure 5E**) (**Supplementary Table 3**). Based on
349 the GO terms enrichment analysis of the biological processes using FunRich software, we observed
350 that these proteins, specifically expressed in each condition, were linked to different biological
351 processes (**Figure 5F**). An enrichment of proteins linked to metabolic and energy signaling pathways

352 was found in Frozen and FrozenCell tumoroid conditions compared to Fresh tumoroids, such as AMY1A
353 (amylase, alpha 1A), SDR9C7 (short chain dehydrogenase/reductase family 9C-member 7), CDA
354 (cytidine deaminase) and ARG1 (arginase 1), FKBP (FK506 binding protein), NDUFB10 (NADH
355 dehydrogenase (ubiquinone) 1 beta subcomplex), DDO (D-aspartate oxidase), ADH5 (alcohol
356 dehydrogenase 5 (class III)) and SIAE (sialic acid acetyltransferase). In addition, in the Frozen and
357 FrozenCell condition, we have identified proteins involved in apoptosis like the apoptosis facilitator
358 BCL2L13 (Bcl-2-like protein 13), ATG5 (autophagy related 5) and TXNRD2 (thioredoxin reductase 2). In
359 the Fresh tumoroids, a higher number of proteins linked to cell communication and to signal
360 transduction were identified. Interestingly, some of the specific proteins identified in fresh tumoroids
361 were involved in the immune response, such as GZMB (Granzyme B) expressed by cytotoxic T and NK
362 cells, the cell adhesion molecule Siglec1 (Sialoadhesin) expressed by macrophages, as well as CD163
363 (Cluster Differentiation 163), a marker of anti-inflammatory macrophages and the AMBP (alpha-1
364 microglobulin/bikunin) precursor of a glycoprotein synthesized by lymphocytes. CD177 (CD177
365 molecule), a marker of neutrophil activation, was also identified specifically in fresh tumoroids.

366 In order to better understand the differences linked to the culture conditions, an analysis of the
367 variation of abundance of common proteins to all conditions (2389 proteins) was carried out, using a
368 multiple sample test ANOVA with an FDR of 0.05. A total of 489 proteins showed significantly different
369 expression between the three groups. These specific variations were analyzed by hierarchical
370 clustering and then illustrated by a Heatmap (**Figure 6A**). Six clusters of proteins were identified: one
371 cluster representing the specific underexpressed proteins and one representing the specific
372 overexpressed proteins for each condition (**Supplementary Table 4**). Based on over- and under-
373 expressed proteins, fresh tumoroids and tumoroids made from frozen cells showed more similarities
374 compared to frozen tumoroids, as observed before as well. In order to understand more precisely the
375 impact of these proteins, the analysis of the GOterms of each cluster was carried out with Cytoscape
376 and ClueGO software, allowing to generate the networks connecting the proteins overexpressed (in
377 red) and underexpressed (in green) to their biological processes.

378 The results showed that in the fresh condition (Clusters 3 - 4) (**Figures 6A and 6B**), the signaling
379 pathways linked to cellular respiration and to amino acid metabolism were underexpressed while the
380 frozen tumoroids and FrozenCell tumoroids express more proteins in these two biological processes,
381 which can be explained by the cryopreservation. In another hand, the assembly of the cell-substrate
382 junction and the RNA translation by RNA polymerase appeared to be overexpressed in the Fresh
383 condition compared to the other conditions, involving proteins like ITGB4 (Integrin beta-4). In order to
384 better understand the differences linked to the culture conditions, an analysis of the variation of
385 abundance of common proteins to all conditions (2389 proteins) was carried out, using a multiple
386 sample test ANOVA with an FDR of 0.05. A total of 489 proteins showed significantly different
387 expression between the three groups. These specific variations were analyzed by hierarchical
388 clustering and then illustrated by a Heatmap (**Figure 6A**). Six clusters of proteins were identified: one
389 cluster representing the specific underexpressed proteins and one representing the specific
390 overexpressed proteins for each condition. Based on over- and under-expressed proteins, fresh
391 tumoroids and tumoroids made from frozen cells showed more similarities compared to frozen
392 tumoroids, as observed before as well. In order to understand more precisely the impact of these
393 proteins, the analysis of the GOterms of each cluster was carried out with Cytoscape and ClueGO
394 software, allowing to generate the networks connecting the proteins overexpressed (in red) and
395 underexpressed (in green) to their biological processes.

396 The results showed that in the fresh condition (Clusters 3 - 4) (**Figures 6A and 6B**), the signaling
397 pathways linked to cellular respiration and to amino acid metabolism were underexpressed while the

398 frozen tumoroids and FrozenCell tumoroids express more proteins in these two biological processes,
399 which can be explained by the cryopreservation. In another hand, the assembly of the cell-substrate
400 junction and the RNA translation by RNA polymerase appeared to be overexpressed in the Fresh
401 condition compared to the other conditions, involving proteins like ITGB4 (Integrin beta-4), Macf1
402 (Microtubule-actin cross-linking factor 1), PSMC2-6 (proteins linking with proteasome), KRT14 (keratin
403 14), PLEC (plectin) and VCL (Vinculin). The proteins involved in cell adhesion are overexpressed in the
404 Fresh condition, which can explained by the formation of tumoroids that form their own extracellular
405 matrix and by the cell compaction.

406 For the FrozenCell condition (Clusters 1 - 2) (**Figure 6C**), there is a higher abundance of proteins linked
407 to chromatin remodeling and cellular metabolism as we observed before, some examples of proteins
408 are UBA52 (Ubiquitin-60S ribosomal protein L40) and PSMC1, PSMD5 (26S proteasome non-ATPase
409 regulatory subunit 1-5) proteasome regulatory forms, RAB7A (Ras-related protein Rab-7a), HSPA9-
410 HSPA5- HSPA8 (Endoplasmic reticulum chaperone BiP), DDB1 (DNA damage-binding protein 1), MDH2
411 (Malate dehydrogenase), SLC25A12 (Calcium-binding mitochondrial carrier protein Aralar1). Again, a
412 high metabolic activity that is a consequence of freezing, in addition to the chromatic remodeling that
413 is involved in the cell division cycle, can be linked to a process of multiplication and recovery from
414 freezing that seems important in this condition.

415 Finally, in frozen tumoroids (Clusters 5 - 6) (**Figure 6D**), many proteins related to protein translation,
416 the proteins of the Extracellular matrix assembly, the Vesicle-mediated transport, Protein translation
417 and Protein - RNA nuclear export were found to be overexpressed. We find an overexpression of
418 proteins linked to the transport of extracellular vesicles, vesicle budding from membrane, vesicle
419 targeting, vesicle coating and COPPII coated vesicles cargo such as: ARCN1 (Coatomer subunit beta-
420 delta), AP2A1 (AP-2 complex subunit alpha), DYNC1H1 (Cytoplasmic dynein 1 heavy chain 1), AP2B1
421 (AP complex subunit beta), ANXA7 (Annexin A7), SEC13 (Protein SEC13 homolog), among others. In
422 addition we can observe an overexpression of the biological processes linked to Protein translation,
423 Protein-RNA nuclear export and Telomerase RNA localization. For example, different proteins of
424 Eukaryotic translation initiation factor (4A-III, 3 subunit A, 3 subunit L, 3 subunit B, 3 subunit E, among
425 others) and 40S and 60S ribosomal protein (RPL10, RPL13A, RPL14, RPL15, RPS11, RPS13, RPS18,
426 RPS28, RPS3, RPS8, RPSA) are overexpressed in the Protein translation biological process. These
427 biological processes show a dysfunction in the translation pathways that we know contribute to cancer
428 progression, for example, in the deregulation of ncRNAs that leads to aberrant protein translation in
429 cancers(29).

430
431 On the contrary, the underexpressed proteins are related to the metabolism of amino acids or
432 nucleotides, negative regulation of cytokines, immune effector process, and the organization of the
433 cytoskeleton, cell adhesion and death. Different metabolic pathways were touched, such as
434 dicarboxylic acid metabolic process, purine ribonucleotide biosynthetic process, pyruvate metabolic
435 process, generation of precursor metabolites and energy. Regarding the organization of the
436 cytoskeleton and cell adhesion, different isoforms of laminin, collagen, catenin and Coronin-1B were
437 found to be under expressed in this condition. Apoptosis and cell death proteins were also found under
438 expressed as CYP1B1 (Cytochrome P450), HSPA1 (Heat shock protein 75 kDa), ARL6IP5 (PRA1 family
439 protein 3), TRAP1 (TNF receptor associated protein 1), among others. In addition, we have identified
440 underexpressed proteins linked to a regulation of cytokines and to the immune effector process, in
441 which we find proteins such as: CD44 (CD44 antigen), thrombospondin-1, SAMHD1 (Deoxynucleoside
442 triphosphate triphosphohydrolase SAMHD1), TINAGL1 (Tubulointerstitial nephritis antigen like 1), GAA
443 (Alpha glucosidase), LGALS9 (Galectin), among others.

444
445 The Cytoscape and ClueGO analysis shows that Fresh and FrozenCell conditions have limited amount
446 of underexpressed and overexpressed proteins, while frozen condition shows three time more

447 proteins with significant variation. On the other side, even if the FrozenCell is closer to Fresh Tumoroids
448 than Frozen condition, the degree of similarity stays high.

449 **3.4. The proteome of canine mammary tumoroids is very similar to the tumor they originate and** 450 **therefore represent a faithful breast cancer model.**

451 We next wanted to determine whether the three different types of tumoroids were similar to the
452 tumor of origin, since the tumoroids will be used as a model of breast cancer.

453 For this, a Venn diagram (**Figure 7A**) was made and showed the number of common and unique
454 proteins in all conditions (**Supplementary Table 5**). It can be observed that a majority of proteins were
455 identified in all three conditions of culture (2138 proteins, representing 74% of all proteins). However,
456 there were specific proteins for each condition especially in the original tumor: 4 identified specifically
457 in fresh tumoroids, 15 in frozen tumoroids, 15 in tumoroids made from frozen cells and 153 specific
458 proteins that were found specifically in the tumor. These 153 proteins are involved in different
459 biological processes such as Cell growth and/or maintenance, Cell communication, Signal transduction
460 and Immune response (**Figure 7B**). Interestingly, an immunological profile can be observed in the
461 tumor compared to the tumoroids. We found many proteins involved in the complement signaling
462 pathway (complement factor I, complement component 4 binding protein, complement component
463 5, complement component 7 and complement component 8) that are involved in immunological
464 response and phagocytosis and found overexpressed in different types of cancer, such as breast
465 cancer(30). In addition, proteins such as CD93 molecule, CD34 molecule, C-type lectin domain family
466 4 member G, haptoglobin and joining chain of multimeric IgA and IgM have been identified and are all
467 implicated in immune response. The AOC3 (amine oxidase, copper containing 3) protein was also
468 identified, and has been recently described to play a role in the reduction of immune cell recruitment
469 and impacting the promotion and progression of lung cancer(31).

470 To better understand the differences between tumor and tumoroids, an analysis of the variation of
471 abundance of common proteins was carried out, using a multiple sample test ANOVA with an FDR of
472 0.05. A total of 512 proteins showed significantly different expression between the four groups. These
473 specific variations were analyzed by hierarchical clustering and then illustrated by a Heatmap (**Figure**
474 **7C**). The HeatMap shows only small variations between the three types of tumoroids. Frozen
475 tumoroids were more different compared to the two other culture conditions confirming the previous
476 results. Interestingly, a small cluster of overexpressed proteins was observed in Tumor, Fresh and
477 FrozenCell tumoroids, while down-expressed in Frozen tumoroids. This result shows again that the
478 conditions more similar to the tumor of origin are the Fresh and FrozenCell tumoroids.

479 We next focused on the two clusters that showed the significant differences between the tumor of
480 origin and the tumoroids (**Supplementary Table 6**). The Heat Map shows two clusters of proteins over-
481 or down-expressed in Tumor compared to the different tumoroids. Functional annotation and
482 characterization of these two clusters of proteins were performed using FunRich software. The results
483 showed that the biological processes underexpressed in the tumor compared to tumoroids are
484 different processes involved in metabolism, transport, energy pathways, apoptosis and signal
485 transduction (**Figure 7D**). On the contrary, we can observe that proteins overexpressed in the tumor
486 compared to tumoroids are involved in cell growth and maintenance, cytoskeleton organization, cell
487 communication, signal transduction and immune response (**Figure 7E**). These results confirm that in
488 tumoroids we find a higher metabolic activity, especially in frozen tumoroids as demonstrated above.
489 In addition, we can observe apoptotic proteins such as BCL2-associated athanogene 6, heat shock
490 60kDa protein 1, PH domain and leucine rich repeat protein phosphatase 2, cell cycle and apoptosis
491 regulator 2, underexpressed in the tumor and consequently overexpressed in the tumoroids. In

492 addition, in the tumor we can find an important proliferative profile demonstrated by the
493 overexpression of proteins involved in cell communication and linked to the organization of the
494 cytoskeleton and cell growth (actin beta-like 2, collagen type VI, tubulin, beta 4B class IVb, lamin A/C,
495 actin alpha 2, actin related protein, among others). Finally, we can find an immune profile more
496 present in the tumor of origin.

497 **3.5 Canine mammary tumoroids can be used to test human drugs and cryopreservation of tumoroids** 498 **does not impact drug response.**

499 In order to evaluate canine mammary tumoroids as useful tools for translational *in vitro* drug screening
500 studies, we performed cell viability assays in presence of a chemotherapeutic agent used in human
501 medicine, Paclitaxel. Tumoroids were treated with Paclitaxel for 7 days before cell viability was
502 measured. Representative images of tumoroids derived from TM-05 tumor are shown in **Figure 8A**
503 demonstrating drug sensitivity depending on the drug concentration. Using 6 concentrations of
504 Paclitaxel, we generated dose-response curves (**Figure 8B**). First, we could demonstrate that tumoroids
505 derived from fresh canine mammary tumors responded well to Paclitaxel with an IC50 ranging from
506 0.1 and 1 μ M. 0.1 μ M Paclitaxel was needed to kill 50% of tumor cells for TM-04 and TM-06 while
507 around 1 μ M was needed for TM-05 demonstrating higher resistance to Paclitaxel.

508 We next compared the Paclitaxel response between fresh tumoroids, frozen tumoroids and tumoroids
509 made from frozen cells in order to verify whether cryopreserved tumoroids could represent faithful
510 models for drug testing. Killed curves from these three culture conditions were similar for the three
511 tumors tested (**Figure 8B**). As we have observed before with the proteomic analysis, fresh tumoroids
512 and tumoroids derived from frozen cells were the most similar in term of Paclitaxel responses.
513 Nonetheless, tumoroids derived from frozen cells appear to become slightly more resistant at higher
514 concentrations of Paclitaxel (**Figure 8A and B**) compared to fresh tumoroids. Indeed, an increase of
515 viability of tumoroids derived from frozen cells can be observed for each tumor at a concentration of
516 100 μ M. A 50% viability of tumoroids was measured in this condition while only 35% of cells were
517 viable in fresh tumoroids (**Figure 8B**). Finally, the response to Paclitaxel of frozen tumoroids appears
518 to be slightly different compared to the two other conditions, even if not significant. For TM-04 and
519 TM-06, fresh tumoroids and tumoroids made from frozen cells seem to be more sensitive whatever
520 the concentration of paclitaxel used compared to frozen tumoroids. For TM-05, the three curves are
521 more similar. A 50% viability decrease of fresh tumoroids and tumoroids made from frozen cells is
522 observed between 0.1 to 1 μ M of drug while between 1 and 10 μ M of Paclitaxel are needed to kill 50%
523 of tumor cells in the frozen tumoroids condition (**Figure 8B**). In the end, we have shown that Paclitaxel
524 response between luminal subtype CMT tumoroids and human breast tumoroids was similar with
525 0.1 μ M of Paclitaxel needed to kill 50% of tumor cells (**Figure 8C**).

526 In conclusion, canine tumoroids respond well to a chemotherapeutic agent used in human medicine.
527 The way the tumoroids are preserved has little impact on drug response. It seems, however, that
528 tumoroids made from frozen cells best mimic the drug response of fresh tumoroids.

529 **4 Discussion**

530 Tumoroids provide an alternative to pre-clinical animal experiments and can help predict tumor
531 response to therapy and screen new drugs. Until now, breast cancer tumoroids have been derived
532 mainly from murine and human tissues(3,32). However, murine tumors do not reliably reflect the
533 human pathology and the use of human tumors faces several challenges such as ethical issues and the
534 difficulty to access sufficient amount of fresh tissues to culture tumoroids, thus limiting high-
535 throughput screening. In the present study, we have established the culture of canine mammary

536 tumoroids in order to develop a biobank which could be used to provide a better comprehension of
537 breast cancer pathogenesis and for large scale drug screening and therapeutic development for both
538 veterinary and human medicine. In fact, dogs develop naturally numerous tumors in the presence of a
539 functioning immune system that have similar features to human cancers(6,33–35). CMT are the most
540 commonly diagnosed cancer in female dogs (50% of all cancers), which is a significant advantage since
541 a large cohort of dogs could be recruited for preclinical studies.

542 Subtype classification of CMT has been investigated in a number of studies using IHC expression of PR,
543 ER and HER2. Several distinct subtypes were identified including luminal A (14.3%), luminal B (9.4%)
544 and triple negative (76.3%), while no HER2-overexpressing CMT were observed (7). Of the 6 dog
545 patients included in the study, 4 tumors were of triple-negative subtype while 2 tumors were of luminal
546 subtype, representing 67% of triple negative tumors and 33% of luminal tumors, which is consistent
547 with previous findings. In human, as in dogs, the triple negative subtype is more aggressive leading to
548 shorter survival rates compared to other tumors (33). Since therapeutic options for this subtype are
549 limited, developing a reliable model to discover new effective treatments is highly needed.

550 We successfully generated tumoroids from CMT with a success rate of more than 94%. For comparison,
551 in a recent study, human tumoroid establishment efficiency was around 40% for triple negative
552 subtype(36). This difference can be explained by a higher amount of tissue which can be obtained from
553 canine tumors, leading to high success rates. These tumoroids keep similar histological features as the
554 original tumors as well as the same molecular subtype. Moreover, by a global proteomic analysis, we
555 have shown that tumoroids were highly similar to the original tumor, 74% of proteins were identified
556 in common between tumoroids and tumor. The tumor specific signature is of course due to a higher
557 cellular diversity in the primary tumor compared to tumoroids, as demonstrated by the over-
558 expression of immune related proteins such as proteins of the complement pathway. On the contrary,
559 an enriched metabolic signature is noticed in tumoroids compared to the primary tumor, which can be
560 explained by the stress of the culture triggering a higher cellular activity. Nevertheless, a high degree
561 of similarity is kept between tumor and tumor-derived tumoroids. Interestingly, a recent study found
562 that the main pathways that were enriched in breast cancer were linked to cell communication, cell
563 growth and maintenance and signal transduction, which correlate well with our findings and is an
564 additional proof that CMT are highly similar to human breast cancer(37).

565 Recently many tumoroid biobanks have emerged from different cancer types(38). Many of these
566 studies have demonstrated that tumoroids preserve the genetic composition of the original tumor.
567 However, the extent of molecular drift at later passage and after cryopreservation has been relatively
568 low studied so far. In the presented study, we have compared histologic and molecular features
569 (marker-based subtype and global proteome) as well as therapeutic response of tumoroids maintained
570 in culture without cryopreservation (fresh tumoroids), put in culture after cryopreservation (frozen
571 tumoroids) or developed from frozen cells (issued from the initial tumor, frozen cell tumoroids). We
572 found that from a morphological point of view, the three types of tumoroids were similar and kept the
573 same architecture and growth rates. The CMT subtype was also maintained after cryopreservation.
574 We have also found that the type of culture or the number of passages did not impact too much the
575 proteome of tumoroids. Indeed, the main variations were observed between tumoroids derived from
576 different tumors rather than between different culture conditions. However, with this global
577 proteomic analysis, we still found that fresh tumoroids and tumoroids made from frozen cells were
578 more similar with a higher proteome diversity compared to frozen tumoroids. A previous study showed
579 that tumor heterogeneity and cell diversity was conserved between fresh tumor tissue and
580 cryopreserved tissue fragments or from cryopreserved cell suspensions (39). In the same study, the
581 authors found that cryopreserved cell suspensions displayed higher correlations to fresh cells

582 compared to tissue fragments. This can therefore explain our observations. Moreover, maintenance
583 of stromal cell populations in tumoroids system is really challenging. At this time, the tumoroids culture
584 system promote the expansion of the tumor cells but do not support the maintenance of immune cells
585 and stromal cells(40). Stromal cells and immune cells are maintained during the first passages and tend
586 to decrease overtime. By using an air-liquid interface to reconstitute the tumor microenvironment,
587 tumoroids integrating immune components were successfully generated but immune cells tend to
588 decline over time(41). Our proteomics results tend to demonstrate this fact, when tumoroids are kept
589 fresh or are made from cells frozen after tumor dissociation, many proteins involved in metabolism,
590 cell communication and immune response were identified. This immune signature was even much
591 more pronounced for fresh tumoroids as demonstrated by the expression of T cell and macrophage
592 markers (Granzyme B, Siglec1 and CD163). These results suggest that the cellular diversity may be
593 higher in fresh tumoroids and tumoroids made from frozen cells compared to cryopreserved
594 tumoroids. Metabolic and stress signatures were enriched in frozen tumoroids, which can be explained
595 by cryopreservation(39).

596 To finish demonstrating that the culture conditions do not impact too much the tumoroids behavior,
597 we have performed a drug response of tumoroids with a known chemotherapy used in human
598 medicine. Paclitaxel response was similar between tumoroids, whatever the condition (fresh or
599 cryopreserved). We however observed that cryopreserved tumoroids were slightly more resistant to
600 Paclitaxel, reflected by a higher concentration of drug needed to kill 50% of cancer cells. These results
601 corroborate our previous observations. Nevertheless, CMT tumoroids are sensitive to a human
602 chemotherapy in a dose dependent manner with a similar response as human breast tumoroids.

603 **5 Conclusions**

604 In conclusion, for the first time, dog mammary tumoroids were produced from heterogeneous tumors.
605 The tumoroids recapitulated the tumor histologic and molecular heterogeneities. Cryopreservation,
606 which is often used for bio banking, did not seem to affect the molecular features and drug response
607 of tumoroids. Nevertheless, we showed that cryopreservation of tumor cells after dissociation seem
608 to best mimic the fresh tumoroids, with a higher molecular diversity. Canine tumoroids can be used to
609 screen human drugs without limitations about tissue availability allowing large scale production.
610 However, to make tumoroids even closer to the primary tumor, it is necessary to develop tumoroid
611 models including stromal components such as immune cells which are lost during traditional tumoroids
612 culture.

613 **Acknowledgements**

614 The authors would like to thank Dr Alexandra Deviers, veterinary pathologist, for histopathological
615 classifications of the canine mammary tumors used in the study and Dr Emmanuelle Cottin,
616 veterinarian who provided us part of the tumor samples.

617 **Funding**

618 This research was funded by Institut National de la Santé de la recherche Médicale (Inserm) and with
619 financial support from ITMO Cancer AVIESAN (Alliance Nationale pour les Sciences de la Vie et de la
620 Santé, National Alliance for Life Sciences & Health) within the framework of the Cancer Plan.

621 **Availability of data and materials**

622 The mass spectrometry proteomics datasets generated and analyzed during the current study have
623 been deposited to the ProteomeXchange Consortium via the PRIDE partner repository and are
624 available with dataset identifier PXD031440.

625 **Authors' contributions**

626 ARR, MD and MS wrote the manuscript. MD and MS were responsible for the concept and design of
627 the overall study and interpretation of the data. ARR and MD were involved in the experimental design,
628 acquisition of the data and analysis and interpretation of the data. SA and EB provided technical
629 assistance and guidance. NH, AR and DT provided the samples. MD, MS and IF supervised the project
630 and provided critical revision of manuscript. MD, MS, IF and DT have obtained funding. All authors read
631 and approved the final manuscript.

632 **Ethics approval and consent to participate**

633 All animal and human studies were reviewed and approved by the local ethics committees, as detailed
634 in the Materials and Methods section.

635 **Competing interests**

636 The authors declare that they have no competing interests.

637

638

639

640

641

642

643

644

645

646

647

648

649

650

651

652

653

654

655

656 **Figure legends**

657 **Figure 1: Breast cancer tumoroids culture established from canine patient.** (A) Diagram presenting
658 the strategy used to culture tumoroids from a canine mammary tumor. (B) Representative images of
659 canine tumoroids at different time points of culture. Scale bar (200 μ m) is indicated. (C) H&E staining
660 comparison between tumoroids and the tumor of origin for three different dog patients.

661 **Figure 2: Study of canine mammary tumoroids drift.** (A) Diagram showing the strategy used to
662 generate the different types of tumoroids. After tumor digestion, a part of the cells were frozen and
663 then thawed to generate the "Frozen Cell Tumoroids". The remaining cells were used to generate the
664 "Fresh tumoroids". A part of these tumoroids were cryopreserved and then thawed, corresponding to
665 the "Frozen Tumoroids". The three types of tumoroids were compared at the same time point post-
666 culture at date 1 (4-5 weeks) or date 2 (6-7 weeks). (B) Representative images of the three types of
667 canine tumoroids at passage one, two and three after Date 1. Scale bar (200 μ m) is indicated. (C) H&E
668 staining comparison of fresh, frozen and frozen cells tumoroids. Scale bar=100 μ m

669 **Figure 3: Histology and receptor status (ER, PR, HER2) of breast cancer tumoroids.** Comparative
670 histological and immunohistochemical images of breast cancer tumoroids and their original breast
671 cancer tissues.

672 **Figure 4: Proliferative activity of the tumoroids.** Comparative quantification of the percentage of
673 Ki67+ cells in tumoroids (Fresh, Frozen and FrozenCell conditions). The average of the triplicates is
674 shown and error bars mean SD. Proliferation did not differ significantly between the 3 conditions.

675 **Figure 5: Proteomics analysis of CMT tumoroids.** (A) Venn diagram representing specific proteins
676 identified in the Fresh, Frozen and FrozenCell tumoroids at Date 1 and Date 2. (B) Biological processes
677 of the proteins identified in common except in Frozen D1 tumoroids. (C) Matrix correlation studies
678 between the two dates in the tree different conditions. (D) PCA analysis of the proteomics data from
679 the tree different tumoroid conditions. (E) Venn diagram representing specific proteins in the Fresh,
680 Frozen and FrozenCell tumoroids. (F) Funrich biological process distribution of the specific proteins
681 identified in Fresh, Frozen and FrozenCell tumoroids.

682 **Figure 6: Proteomics analysis of Fresh, Frozen and FrozenCells tumoroids.** (A) Hierarchical clustering
683 of the most variable proteins between the 3 conditions (n = 3 for each condition, ANOVA with
684 permutation-based FDR < 0.05). Network of proteins overexpressed (red) or underexpressed (green)
685 in Fresh (B), FrozenCell (C) and Frozen (D) tumoroids and their associated GO terms. The networks
686 were enriched through addition of STRING network to the identified proteins using ClueGO application
687 on Cytoscape.

688 **Figure 7: Proteomics analysis comparing the primary tumor to their derived tumoroids.** (A) Venn
689 diagram representing specific proteins in tumor of origin, Fresh, Frozen and FrozenCell tumoroids. (B)
690 Biological processes of the specific proteins identified in primary tumors using Funrich and ClueGO. (C)
691 Hierarchical clustering of the most variable proteins between the tumor of origin and the 3 tumoroid
692 conditions (n = 3 for each condition, ANOVA with permutation-based FDR < 0.05). Biological processes
693 distribution of underexpressed (D) and overexpressed (E) proteins in tumors compared to tumoroids
694 using Funrich and Cluego.

695 **Figure 8: Drug response of canine and human tumoroids to Paclitaxel.** (A) Representative bright field
696 images showing the morphology of the three types of tumoroids after 7 days treatment with Paclitaxel
697 at different concentrations. Scale bar (100 μ m) is indicated. (B) Quantification of the tumoroids viability
698 following Paclitaxel treatment. Tumoroids were generated from three different canine mammary

699 tumors (TM-04, TM-05 and TM-06) and drug response was compared between fresh, frozen and frozen
700 cell tumoroids. (C) Tumoroids were generated from human and canine mammary tumors and drug
701 response was compared between human and canine tumoroids. Different concentrations of drug were
702 used and compared to non-treated tumoroids. Data are the means \pm SD.

703 **Supplementary Figure 1:** Histology and receptor status (ER, PR, HER2) of the 6 canine mammary
704 tumors used in the study.

705 **Supplementary Figure 2:** Immunofluorescence images of Ki67 stained canine mammary tumors.

706 **Supplementary Table 1:** Summary table of canine tumors used in the study.

707 **Supplementary Table 2:** List of proteins in the Venn diagram representing proteins identified in Fresh,
708 Frozen, and FrozenCell tumoroids at date 1 and date 2.

709 **Supplementary Table 3:** List of proteins in the Venn diagram representing proteins in the Fresh, Frozen
710 and FrozenCell tumoroids.

711 **Supplementary Table 4:** List of proteins in the 6 clusters identified in the Hierarchical clustering of the
712 most variable proteins between the Fresh, Frozen and FrozenCell conditions.

713 **Supplementary Table 5:** List of proteins in the Venn diagram representing proteins in the Tumor, Fresh,
714 Frozen and FrozenCell tumoroids conditions.

715 **Supplementary Table 6:** List of proteins in the 2 clusters identified in the Hierarchical clustering of the
716 most variable proteins between the Tumor, Fresh, Frozen and FrozenCell tumoroids conditions.

717

718 **6 References**

- 719 1. Wong CH, Siah KW, Lo AW. Estimation of clinical trial success rates and related parameters.
720 Biostatistics [Internet]. 2019 [cited 2019 Oct 17];20(2):273–86. Available from:
721 <http://www.ncbi.nlm.nih.gov/pubmed/29394327>
- 722 2. Broutier L, Mastrogiovanni G, Versteegen MM, Francies HE, Gavarró LM, Bradshaw CR, et al.
723 Human primary liver cancer-derived organoid cultures for disease modeling and drug
724 screening. Nat Med [Internet]. 2017 Dec [cited 2019 Sep 10];23(12):1424–35. Available from:
725 <http://www.ncbi.nlm.nih.gov/pubmed/29131160>
- 726 3. Sachs N, de Ligt J, Kopper O, Gogola E, Bounova G, Weeber F, et al. A Living Biobank of Breast
727 Cancer Organoids Captures Disease Heterogeneity. Cell. 2018 Jan 11;172(1–2):373–386.e10.
- 728 4. Nuciforo S, Fofana I, Matter MS, Blumer T, Calabrese D, Boldanova T, et al. Organoid Models
729 of Human Liver Cancers Derived from Tumor Needle Biopsies. Cell Rep [Internet]. 2018 Jul 31
730 [cited 2019 Sep 10];24(5):1363–76. Available from:
731 <http://www.ncbi.nlm.nih.gov/pubmed/30067989>
- 732 5. Lee SH, Hu W, Matulay JT, Silva M V., Owczarek TB, Kim K, et al. Tumor Evolution and Drug
733 Response in Patient-Derived Organoid Models of Bladder Cancer. Cell. 2018 Apr 5;173(2):515-
734 528.e17.
- 735 6. Nguyen F, Peña L, Ibisch C, Loussouarn D, Gama A, Rieder N, et al. Canine invasive mammary
736 carcinomas as models of human breast cancer. Part 1: natural history and prognostic factors.
737 Breast Cancer Res Treat [Internet]. 2018 [cited 2019 Oct 17];167(3):635–48. Available from:
738 <http://www.ncbi.nlm.nih.gov/pubmed/29086231>

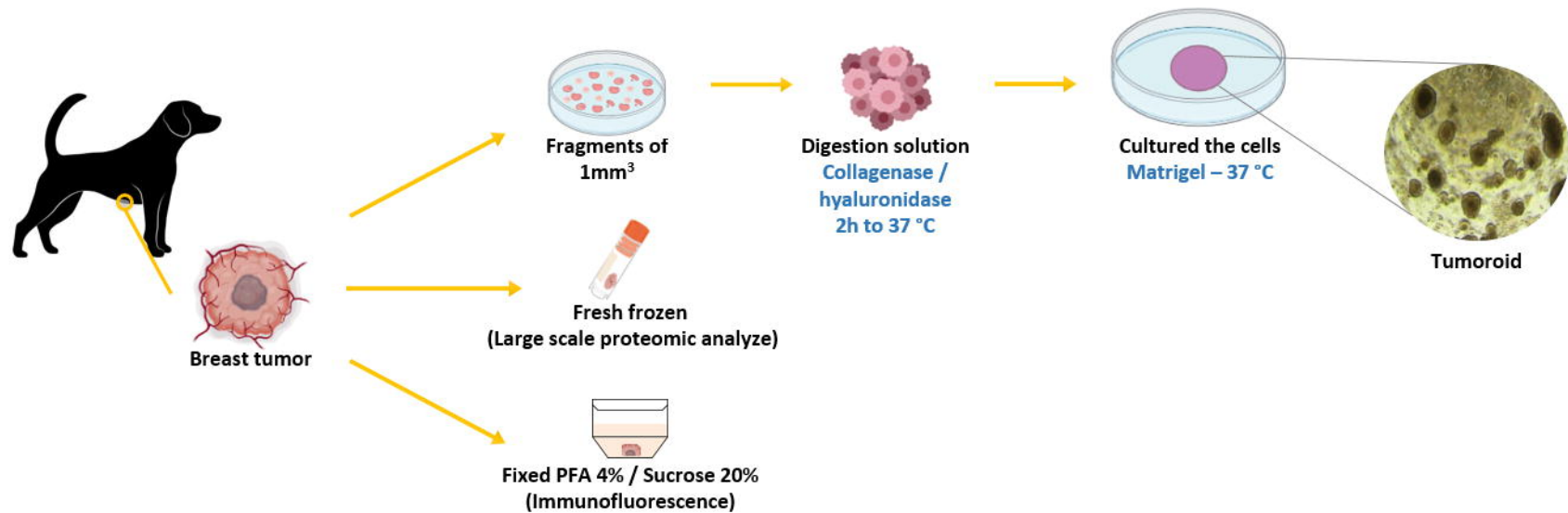
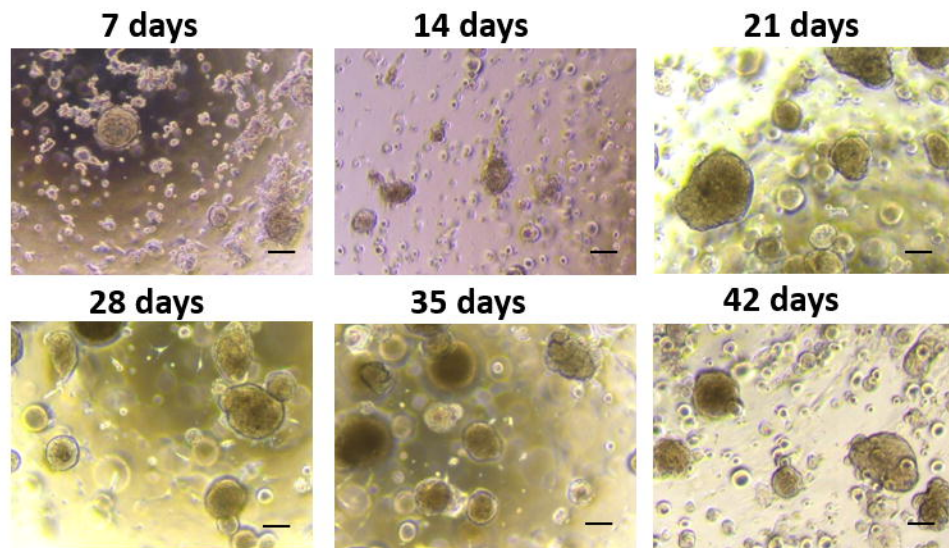
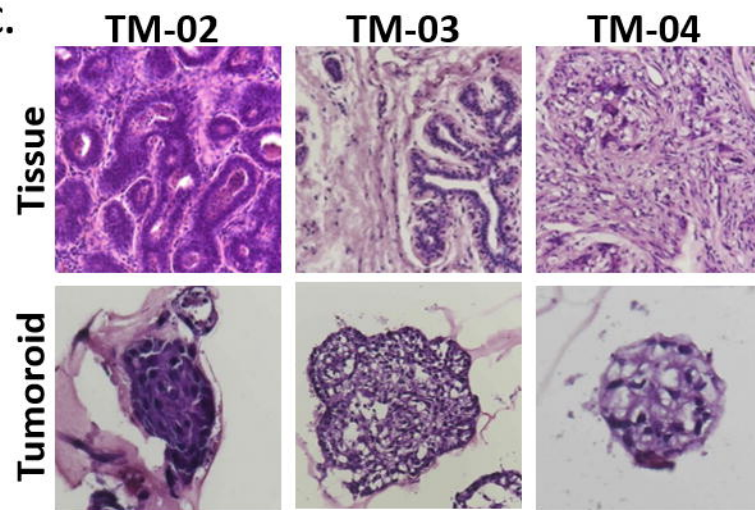
- 739 7. Abadie J, Nguyen F, Loussouarn D, Peña L, Gama A, Rieder N, et al. Canine invasive mammary
740 carcinomas as models of human breast cancer. Part 2: immunophenotypes and prognostic
741 significance. *Breast Cancer Res Treat* [Internet]. 2018 [cited 2019 Oct 17];167(2):459–68.
742 Available from: <http://www.ncbi.nlm.nih.gov/pubmed/29063312>
- 743 8. Dorn CR, Taylor DON, Schneider R, Hibbard HH, Klauber MR. Survey of animal neoplasms in
744 alameda and contra costa counties, california. ii. cancer morbidity in dogs and cats from
745 alameda county. *J Natl Cancer Inst*. 1968;40(2):307–18.
- 746 9. Dobson JM, Samuel S, Milstein H, Rogers K, Wood JLN. Canine neoplasia in the UK: estimates
747 of incidence rates from a population of insured dogs. *J Small Anim Pract* [Internet]. 2002 Jun
748 [cited 2019 Oct 17];43(6):240–6. Available from:
749 <http://www.ncbi.nlm.nih.gov/pubmed/12074288>
- 750 10. Egenvall A, Bonnett BN, Ohagen P, Olson P, Hedhammar A, von Euler H. Incidence of and
751 survival after mammary tumors in a population of over 80,000 insured female dogs in Sweden
752 from 1995 to 2002. *Prev Vet Med* [Internet]. 2005 Jun 10 [cited 2019 Oct 17];69(1–2):109–27.
753 Available from: <http://www.ncbi.nlm.nih.gov/pubmed/15899300>
- 754 11. MacEwen EG. Spontaneous tumors in dogs and cats: Models for the study of cancer biology
755 and treatment. *CANCER METASTASIS Rev*. 1990 Sep;9(2):125–36.
- 756 12. Queiroga FL, Raposo T, Carvalho MI, Prada J, Pires I. Canine mammary tumours as a model to
757 study human breast cancer: Most recent findings. Vol. 25, *In Vivo*. 2011. p. 455–65.
- 758 13. Michałowska M, Winiarczyk S, Adaszek Ł, Łopuszyński W, Grądzki Z, Salmons B, et al. Phase I/II
759 clinical trial of encapsulated, cytochrome P450 expressing cells as local activators of
760 cyclophosphamide to treat spontaneous canine tumours. *PLoS One* [Internet]. 2014 [cited
761 2019 Oct 17];9(7):e102061. Available from: <http://www.ncbi.nlm.nih.gov/pubmed/25028963>
- 762 14. T U, M S, S N, K U, Y N, T H, et al. Establishment of a dog primary prostate cancer organoid
763 using the urine cancer stem cells. *Cancer Sci* [Internet]. 2017 Dec 1 [cited 2021 Nov
764 2];108(12):2383–92. Available from: <https://pubmed.ncbi.nlm.nih.gov/29024204/>
- 765 15. Kramer N, Pratscher B, Meneses AMC, Tschulenck W, Walter I, Swoboda A, et al. Generation of
766 Differentiating and Long-Living Intestinal Organoids Reflecting the Cellular Diversity of Canine
767 Intestine. *Cells* 2020, Vol 9, Page 822 [Internet]. 2020 Mar 28 [cited 2021 Nov 2];9(4):822.
768 Available from: <https://www.mdpi.com/2073-4409/9/4/822/htm>
- 769 16. Ambrosini YM, Park Y, Jergens AE, Shin W, Min S, Atherly T, et al. Recapitulation of the
770 accessible interface of biopsy-derived canine intestinal organoids to study epithelial-luminal
771 interactions. *PLoS One* [Internet]. 2020 Apr 1 [cited 2021 Nov 2];15(4):e0231423. Available
772 from: <https://journals.plos.org/plosone/article?id=10.1371/journal.pone.0231423>
- 773 17. Chandra L, Borcharding DC, Kingsbury D, Atherly T, Ambrosini YM, Bourgois-Mochel A, et al.
774 Derivation of adult canine intestinal organoids for translational research in gastroenterology.
775 *BMC Biol* [Internet]. 2019 Apr 11 [cited 2021 Nov 2];17(1). Available from:
776 </pmc/articles/PMC6460554/>
- 777 18. C C, S M, E P, MC V, M G, C B, et al. FGF2 and EGF Are Required for Self-Renewal and Organoid
778 Formation of Canine Normal and Tumor Breast Stem Cells. *J Cell Biochem* [Internet]. 2017
779 Mar 1 [cited 2021 Nov 2];118(3):570–84. Available from:
780 <https://pubmed.ncbi.nlm.nih.gov/27632571/>
- 781 19. Botti G, Di Bonito M, Cantile M. Organoid biobanks as a new tool for pre-clinical validation of
782 candidate drug efficacy and safety. *Int J Physiol Pathophysiol Pharmacol* [Internet]. 2021

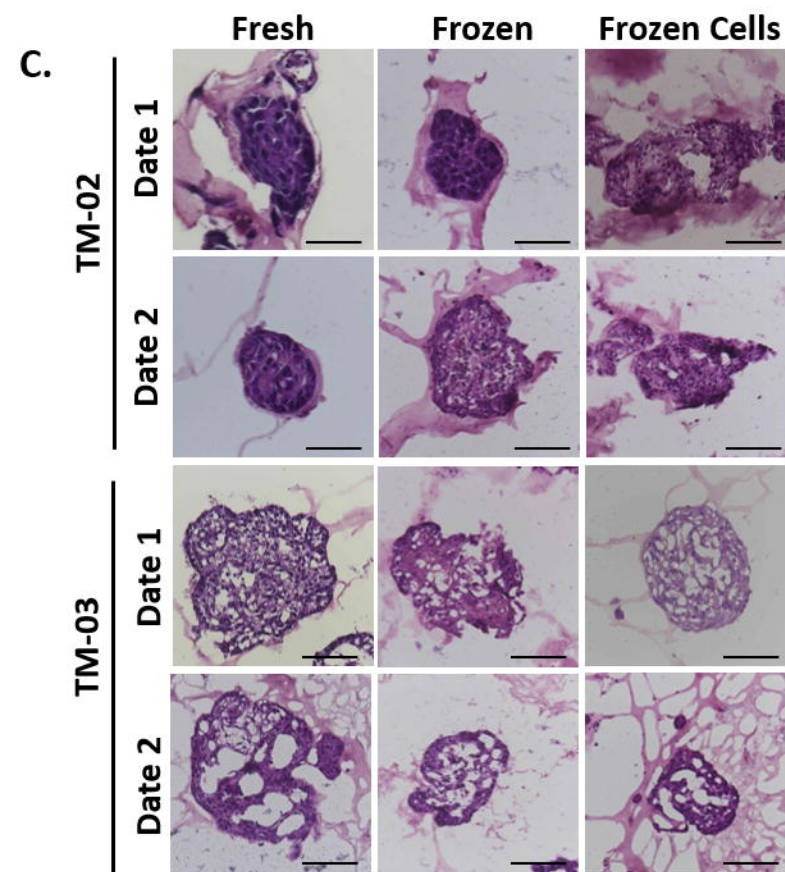
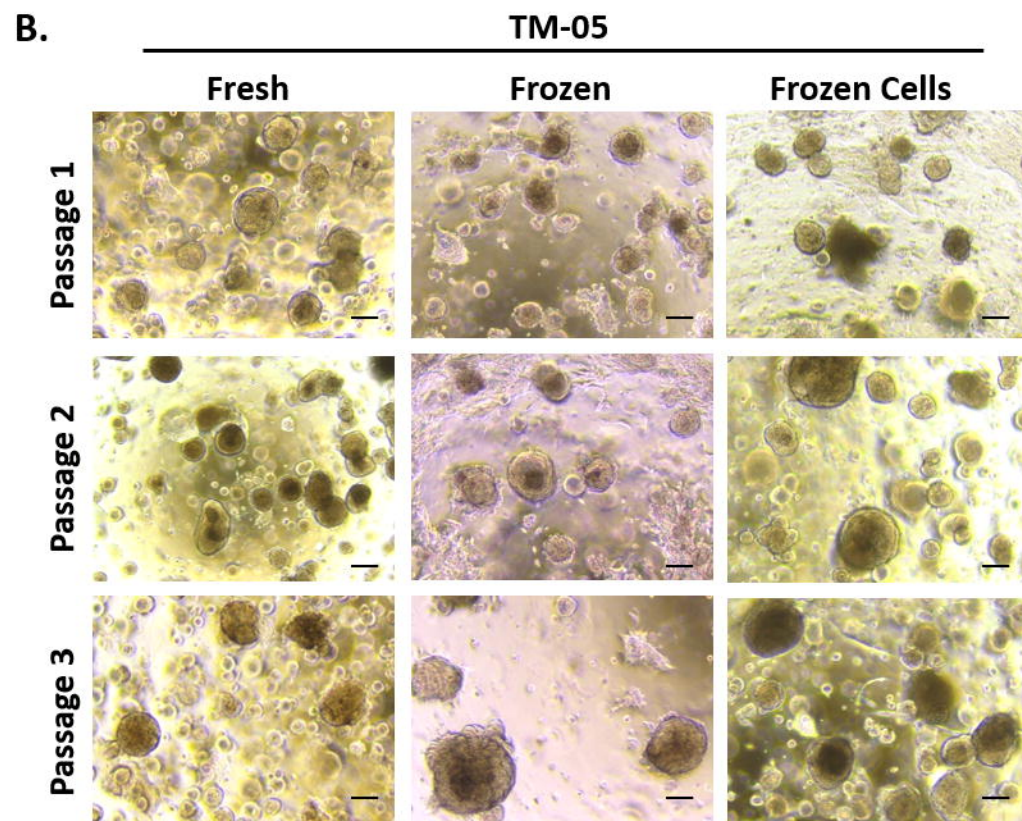
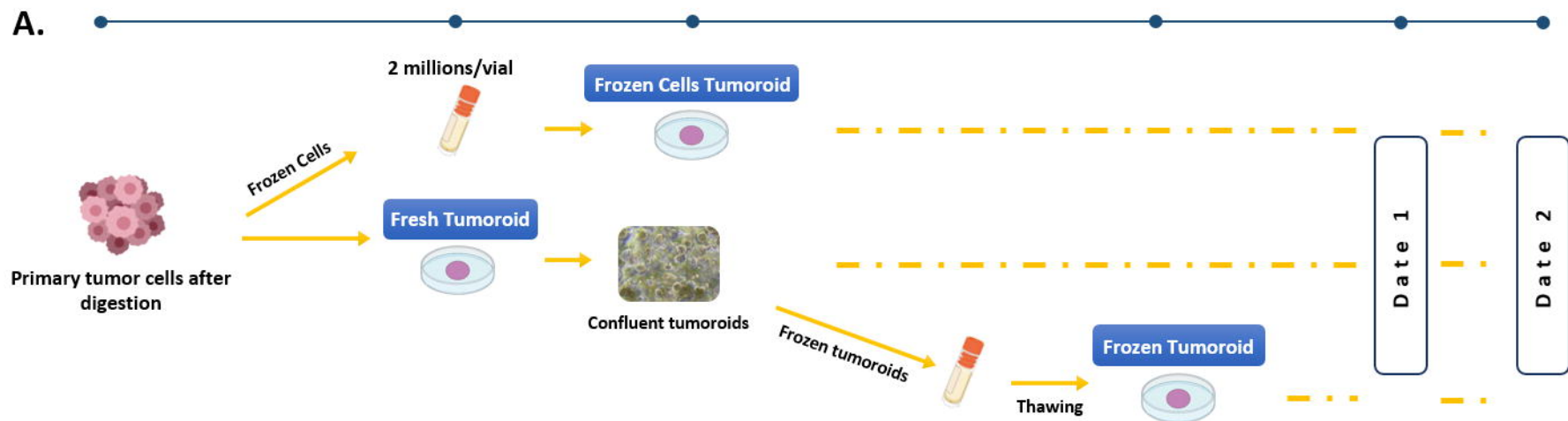
- 783 [cited 2021 Nov 2];13(1):17–21. Available from: <https://clinicaltrials>.
- 784 20. Wiśniewski JR, Zougman A, Nagaraj N, Mann M. Universal sample preparation method for
785 proteome analysis. *Nat Methods*. 2009 May;6(5):359–62.
- 786 21. Cox J, Mann M. MaxQuant enables high peptide identification rates, individualized p.p.b.-
787 range mass accuracies and proteome-wide protein quantification. *Nat Biotechnol* 2008 2612.
788 2008 Nov;26(12):1367–72.
- 789 22. Cox J, Neuhauser N, Michalski A, Scheltema RA, Olsen J V., Mann M. Andromeda: A peptide
790 search engine integrated into the MaxQuant environment. *J Proteome Res*. 2011;10(4):1794–
791 805.
- 792 23. Tyanova S, Cox J. Perseus: A Bioinformatics Platform for Integrative Analysis of Proteomics
793 Data in Cancer Research. *Methods Mol Biol*. 2018;1711:133–48.
- 794 24. Tyanova S, Temu T, Sinitcyn P, Carlson A, Hein MY, Geiger T, et al. The Perseus computational
795 platform for comprehensive analysis of (prote)omics data. *Nat Methods* 2016 139. 2016
796 Jun;13(9):731–40.
- 797 25. Mi H, Huang X, Muruganujan A, Tang H, Mills C, Kang D, et al. PANTHER version 11: expanded
798 annotation data from Gene Ontology and Reactome pathways, and data analysis tool
799 enhancements. *Nucleic Acids Res*. 2017 Jan;45(D1):D183–9.
- 800 26. Szklarczyk D, Franceschini A, Wyder S, Forslund K, Heller D, Huerta-Cepas J, et al. STRING v10:
801 Protein-protein interaction networks, integrated over the tree of life. *Nucleic Acids Res*. 2015
802 Jan;43(D1):D447–52.
- 803 27. Pathan M, Keerthikumar S, Ang CS, Gangoda L, Quek CYJ, Williamson NA, et al. FunRich: An
804 open access standalone functional enrichment and interaction network analysis tool.
805 *Proteomics*. 2015 Aug;15(15):2597–601.
- 806 28. Goldschmidt M, Peña L, Rasotto R, Zappulli V. Classification and grading of canine mammary
807 tumors. *Vet Pathol [Internet]*. 2011 Jan [cited 2019 Oct 22];48(1):117–31. Available from:
808 <http://www.ncbi.nlm.nih.gov/pubmed/21266722>
- 809 29. Song P, Yang F, Jin H, Wang X. The regulation of protein translation and its implications for
810 cancer. *Signal Transduct Target Ther* 2021 61 [Internet]. 2021 Feb 18 [cited 2022 Jan
811 31];6(1):1–9. Available from: <https://www.nature.com/articles/s41392-020-00444-9>
- 812 30. Imamura T, Yamamoto-Ibusuki M, Sueta A, Kubo T, Irie A, Kikuchi K, et al. Influence of the
813 C5a–C5a receptor system on breast cancer progression and patient prognosis. *Breast Cancer*
814 2015 236 [Internet]. 2015 Oct 22 [cited 2022 Jan 31];23(6):876–85. Available from:
815 <https://link.springer.com/article/10.1007/s12282-015-0654-3>
- 816 31. Boyer DS, Rippmann JF, Ehrlich MS, Bakker RA, Chong V, Nguyen QD. Amine oxidase copper-
817 containing 3 (AOC3) inhibition: a potential novel target for the management of diabetic
818 retinopathy. *Int J Retin Vitro [Internet]*. 2021 Dec 1 [cited 2022 Jan 31];7(1). Available from:
819 <https://pubmed.ncbi.nlm.nih.gov/33845913/>
- 820 32. Mohan SC, Lee TY, Giuliano AE, Cui X. Current Status of Breast Organoid Models. *Front Bioeng*
821 *Biotechnol*. 2021 Nov 5;9:1091.
- 822 33. Gray M, Meehan J, Martínez-Pérez C, Kay C, Turnbull AK, Morrison LR, et al. Naturally-
823 Occurring Canine Mammary Tumors as a Translational Model for Human Breast Cancer. *Front*
824 *Oncol*. 2020 Apr 28;10:617.
- 825 34. Uva P, Aurisicchio L, Watters J, Loboda A, Kulkarni A, Castle J, et al. Comparative expression

- 826 pathway analysis of human and canine mammary tumors. *BMC Genomics*. 2009 Mar 27;10.
- 827 35. Abdelmegeed SM, Mohammed S. Canine mammary tumors as a model for human disease
828 (Review). Vol. 15, *Oncology Letters*. Spandidos Publications; 2018. p. 8195–205.
- 829 36. Dekkers JF, van Vliet EJ, Sachs N, Rosenbluth JM, Kopper O, Rebel HG, et al. Long-term culture,
830 genetic manipulation and xenotransplantation of human normal and breast cancer organoids.
831 *Nat Protoc* 2021 164 [Internet]. 2021 Mar 10 [cited 2022 Jan 25];16(4):1936–65. Available
832 from: <https://www.nature.com/articles/s41596-020-00474-1>
- 833 37. Deng JL, Xu YH, Wang G. Identification of potential crucial genes and key pathways in breast
834 cancer using bioinformatic analysis. *Front Genet*. 2019;10(JUL):695.
- 835 38. Lo YH, Karlsson K, Kuo CJ. Applications of Organoids for Cancer Biology and Precision
836 Medicine. *Nat cancer* [Internet]. 2020 Aug 1 [cited 2022 Jan 25];1(8):761. Available from:
837 </pmc/articles/PMC8208643/>
- 838 39. Wu SZ, Roden DL, Al-Eryani G, Bartonicek N, Harvey K, Cazet AS, et al. Cryopreservation of
839 human cancers conserves tumour heterogeneity for single-cell multi-omics analysis. *Genome*
840 *Med* [Internet]. 2021 Dec 1 [cited 2022 Jan 26];13(1):1–17. Available from:
841 <https://genomemedicine.biomedcentral.com/articles/10.1186/s13073-021-00885-z>
- 842 40. Fiorini E, Veghini L, Corbo V. Modeling Cell Communication in Cancer With Organoids: Making
843 the Complex Simple. *Front Cell Dev Biol*. 2020 Mar 18;8:166.
- 844 41. Neal JT, Li X, Zhu J, Giangarra V, Grzeskowiak CL, Ju J, et al. Organoid Modeling of the Tumor
845 Immune Microenvironment. *Cell*. 2018 Dec 13;175(7):1972-1988.e16.

846

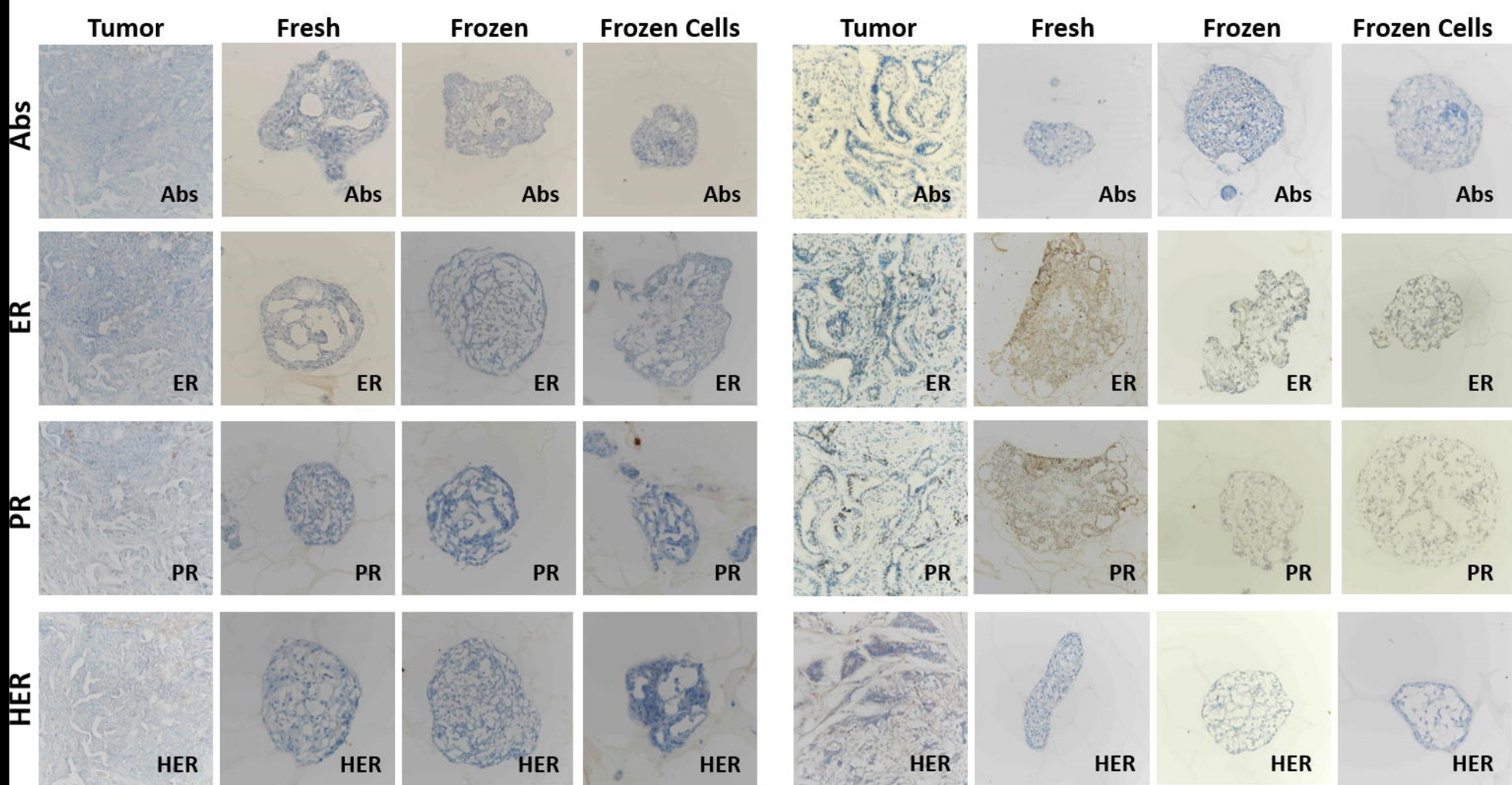
847

A.**B.****C.**

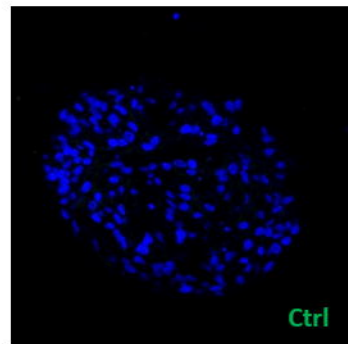
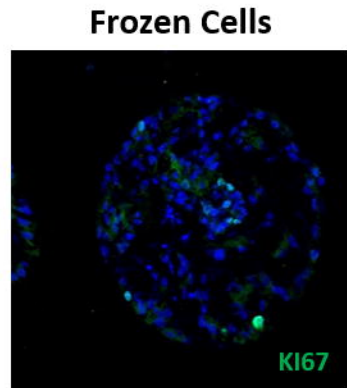
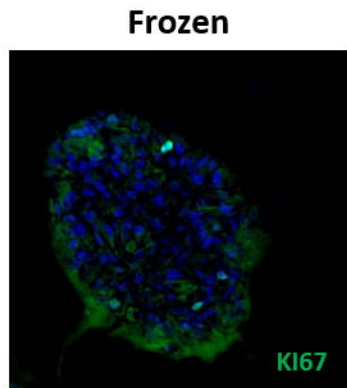
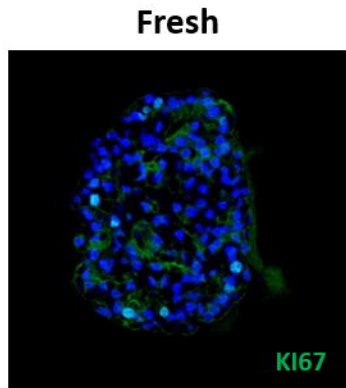
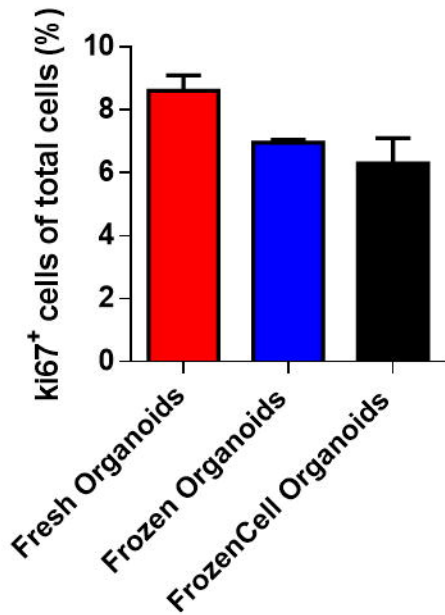


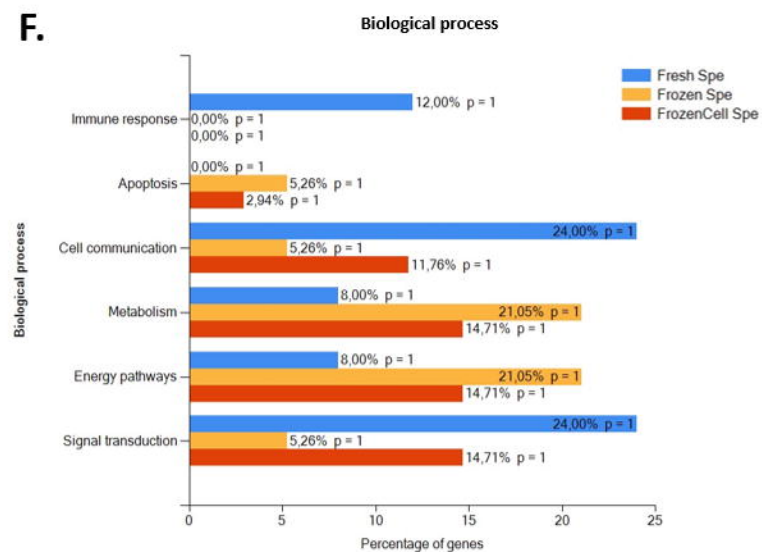
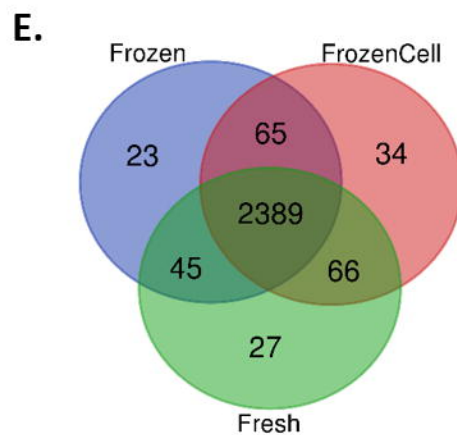
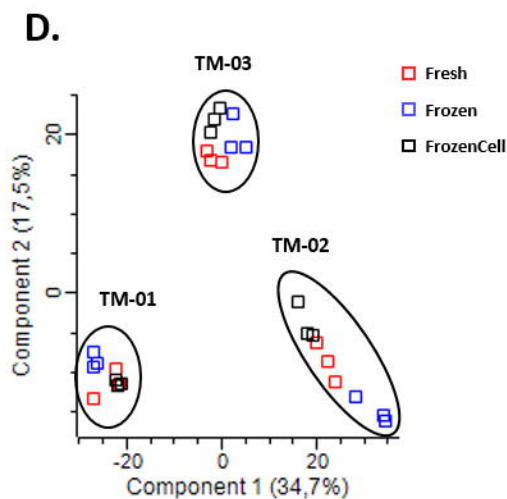
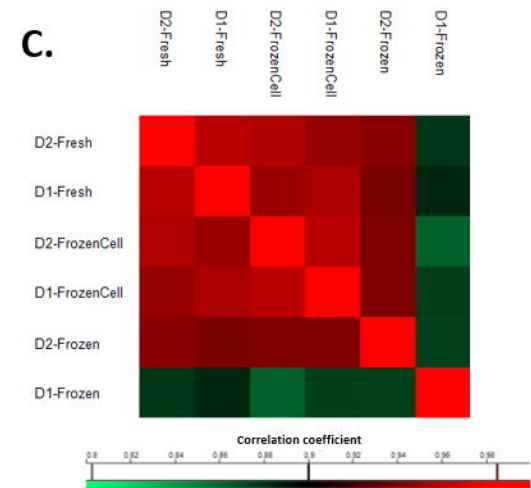
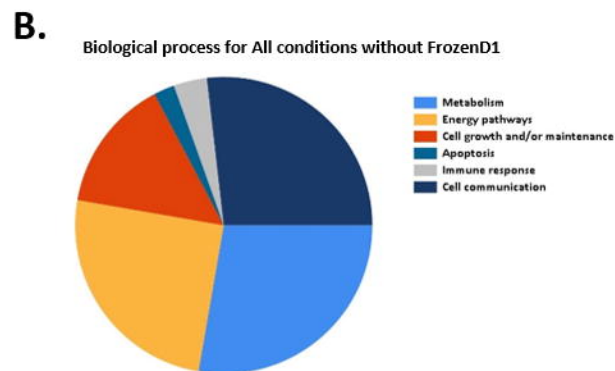
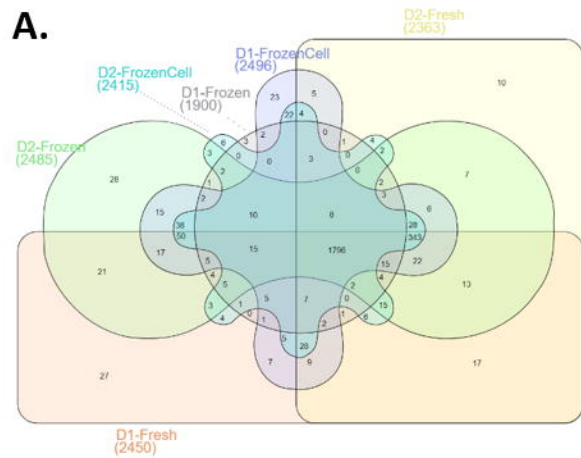
TM-03

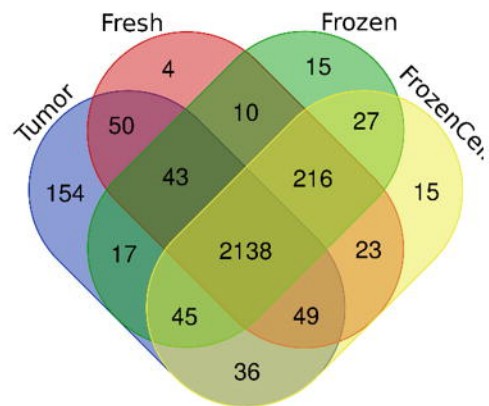
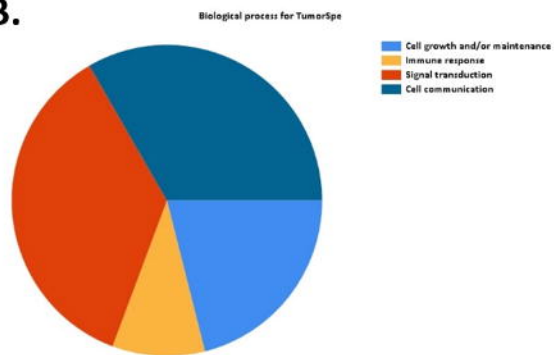
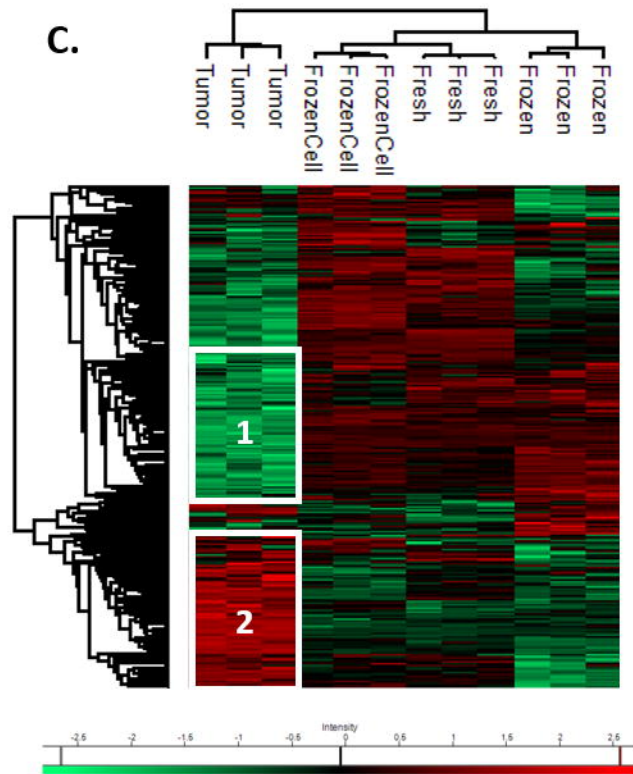
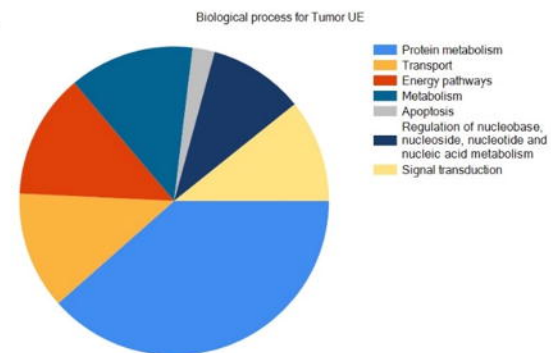
TM-04



TM-05





A.**B.****C.****D.****E.**